1985ApJ...290..140W

THE ASTROPHYSICAL JOURNAL, 290:140–153, 1985 March 1
© 1985. The American Astronomical Society. All rights reserved. Printed in U.S.A.

THE MISSING BULGE GLOBULAR CLUSTERS IN M31: NEW OPTICAL CANDIDATES[1]

A. WIRTH,[2,3] L. L. SMARR,[2,4] AND T. L. BRUNO[5]
Department of Astronomy, University of Illinois
Received 1982 August 2; accepted 1984 September 10

ABSTRACT

We use a new method to attack the question of the "missing" globular clusters in the bulge of M31. Image-processing techniques were used on 13 videocamera fields to obtain an accurate photometric census of stellar objects in M31's bulge down to a limiting B magnitude of 21. This luminosity distribution is compared with the Bahcall-Soneira model of galactic foreground stars. We find a statistically significant excess of bright images in the luminosity range of globular clusters at M31's distance. If our optical candidates prove to be globular clusters, they would double the number of known globular clusters in the surveyed region. The colors of a subsample of our candidates are the same as those of the known globular clusters. We conclude that the previously observed flattening away from a de Vaucouleurs law in the radial distribution of M31 may be an observational selection effect. As an offshoot of this analysis, we find no evidence for very luminous stars in the inner bulge of M31. The lack of such stars indicates that there has not been active star formation (with a normal IMF) in the recent past. Coupled with the existence of many planetary nebulae in the bulge, this may strengthen the case for a galactic wind in M31's bulge.

Subject headings: clusters: globular — galaxies: individual — galaxies: stellar content — stars: formation

I. INTRODUCTION

The bulge of M31 is in many ways the easiest luminous stellar spheroid for us to study. The *Einstein Observatory* discovery (Van Speybroeck *et al.* 1979) of the large, distinct population of point X-ray sources in the M31 bulge has served to heighten interest in the details of its structure. To examine the relation of these X-ray objects to optical sources, a series of photographs of the central part of M31 was obtained with the University of Illinois 1.0 m telescope. One of these, a 103a-O plate taken at the f/7.5 focus, was used to obtain star counts over the M31 field. These counts are presented in Figure 1. There is a clear excess of images brighter than $B \approx 18$ in the central 10′ region, which coincides with the region of the X-ray point sources. Because of the availability of linear, two-dimensional detectors with large dynamic range, it has become possible to make quantitative studies of these stellar images. We have taken advantage of these new techniques to make a magnitude-limited survey of objects within $\sim 10'$ of the nucleus of M31. In this paper, we will discuss the nature of these objects and their implications about the stellar populations present in a typical spiral bulge. Our major result is that we find optical candidates for the "missing" bulge globular clusters. In the second paper of this series, the relation of the objects discovered here to the point X-ray sources will be explored.

[1] This research has been supported in part by grants AST 027-0997 and PHYS 80-01496 from the National Science Foundation and grant NSF 7653 from the National Aeronautics and Space Administration to the University of Illinois.

[2] Visiting Astronomer, Kitt Peak National Observatory, which is operated by the Associated Universities for Research in Astronomy, Inc., under contract with the National Science Foundation.

[3] Now at the Harvard-Smithsonian Center for Astrophysics.

[4] Alfred P. Sloan Foundation Fellow.

[5] Now at RACD/EEV—Hanscom AFB.

II. OBSERVATIONS

Observations were carried out with the KPNO 2.1 m telescope and videocamera on the nights of 1979 October 31 to November 3. During the time the data were taken, the size of the seeing disk (FWHM) varied between 0″.8 and 1″.5 as measured on the videocamera target. Observations were made through the standard videocamera *BVRI* filter set. Exposure times ranged from 7 to 40 minutes. The central field (see Fig. 2) was observed through a neutral density filter to avoid saturation of the Vidicon target by the nucleus of M31. The density and color of this filter were measured by comparison with overlapping regions of fields observed without the filter. Reduction to standard Kron-Cousins *BVRI* magnitudes was done via observations of standard videocamera/CCD fields in NGC 7006, NGC 2419, and M92 (Kitt Peak National Observatory 1980).

By taking full advantage of the large dynamic range and linearity of the videocamera in the data reduction, we have been able to extend the search for stellar and semistellar images in the central region of M31 between 1 and 3 mag fainter than previous studies. Further, accurate photometry has been carried out for most of these images. Table 1 and Figure 2 summarize the observations used to produce the photometry reported here.

We have divided the 13 fields (each 2′ square) into 10 "survey" fields (S1–S10) and three "central" fields (east = E, central = C, west = W). The survey fields were short exposures (7 minutes) in one color (B), whereas the central field exposures were 6 times as long (see Table 1) in two colors (B and I).

III. DATA REDUCTION

All videocamera frames were processed by the standard KPNO software to remove the instrumental signature and average multiple exposures. Further, they were geometrically corrected to allow accurate astrometry and photometry of the

© American Astronomical Society • Provided by the NASA Astrophysics Data System

1985ApJ...290..140W

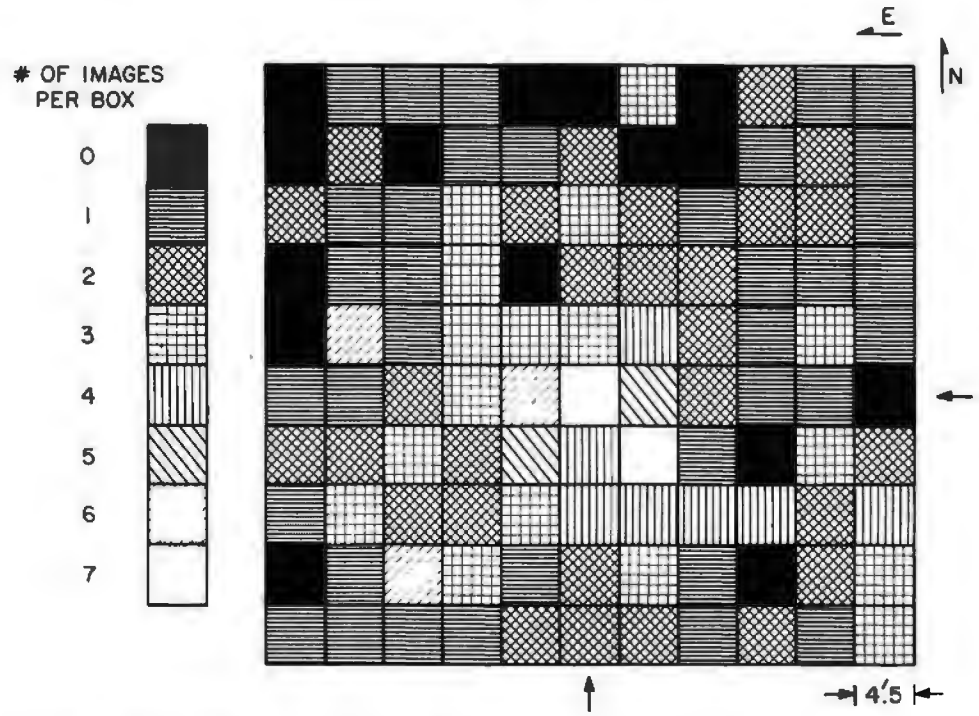


FIG. 1.—Gray-scale representation of star counts from a 103-O plate of M31 obtained with the University of Illinois 1.0 m telescope. All images are brighter than the plate limit of $B \sim 18$. The location of the nucleus is indicated by arrows. Each box is $\sim 4'.5 \times 4'.5$.

images. That is, distortions introduced by the transfer optics and the Vidicon target were removed.

a) Survey Fields

The 10 "survey fields" were sufficiently far from the nucleus to allow the use of simple simulated aperture photometry without undue error. Positions and magnitudes for 154 images appearing in these fields were measured on the Hewlett Packard image-processing system at KPNO using software development by H. Butcher. An aperture size of 4".8 was used. These magnitudes were converted to the B system via observations of the standard fields in M92 and NGC 2419. In order to provide a well-distributed set of positions and magnitudes for further work on the M31 bulge, we list the results of our photometry in Table 2 down to a limiting blue magnitude of 21.

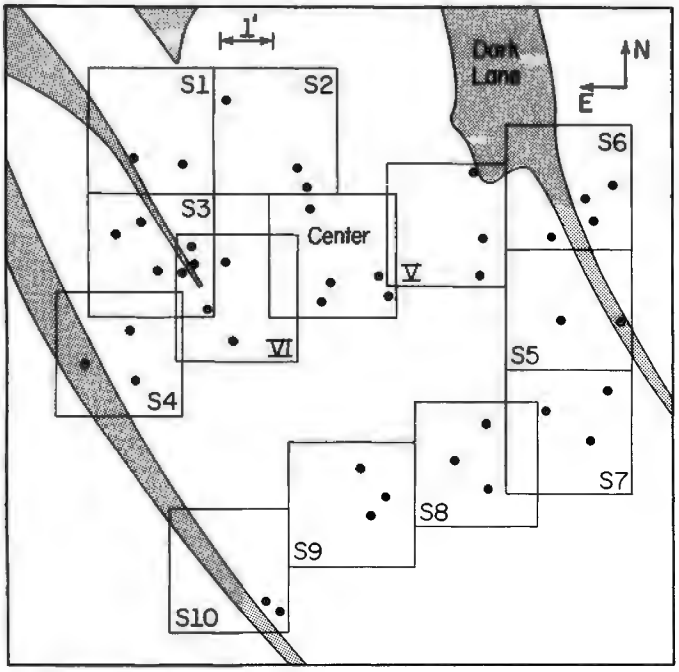


FIG. 2.—The 10 survey fields (S1–S10) and the three central fields (E, C, W) are shown superposed on a finding chart of the brighter stars and large dust lanes of M31.

b) Central Fields

Several attempts were made to use the photometry packages available on the interactive picture-processing system (IPPS) at KPNO to measure the magnitudes of the visible stellar images in the three central fields. It was found that none of these routines gave reliable results because the gradient in the background was very large. Therefore, we were forced to do further processing of these three fields.

Because of the existence of both radial and azimuthal gradients in these fields, it was decided that, rather than attempt to locally fit the "sky," a global model of the bulge background would be made and then subtracted from the raw data, leaving only small-scale image structure. After numerous experiments, it was found that successive median smoothing, first by column then by row, followed by a two-dimensional boxcar smooth yielded a quite star-free and smooth frame. The median smoothings were done with an 11 pixel window (which had the effect of removing sharp peaks), and the box size was 15×15 pixels. This smoothed frame was subtracted from the raw data, leaving only structures with scales of less than ~ 10 pixels. A somewhat similar technique has been used by Strom *et al.* (1981) in their study of M87 globular clusters. The primary difference is that here, because of our smaller image size, we were able to smooth the whole picture, not an extracted subpicture. Figure 3*a* shows the central frame before background removal, while Figure 3*b* is the field after processing.

© American Astronomical Society • Provided by the NASA Astrophysics Data System

1985ApJ...290..140W

TABLE 1

FIELDS OBSERVED

FIELD NAME (see Fig. 2)	EXPOSURES (minutes)			
	B	*V*	*R*	*I*
C	3 × 14, ND[a] 1.0	14, ND 2.0	14, ND 2.0	3 × 14, ND 1.0
W, V	3 × 14	14 + 7	14 + 7	3 × 14
E, VI	3 × 14	14	...	3 × 14
S1	7	...	...	...
S2	7	...	...	...
S3	7	...	...	...
S4	7	...	...	...
S5	7	...	...	...
S6	7	...	...	...
S7	7	...	...	...
S8	7	...	...	...
S9	7	...	...	...
S10	7	...	...	...
FGC 32[b]	7	...	...	7

[a] ND = neutral density filter.
[b] Field centered on globular cluster 32 of M31 consortium: Sargent *et al.* 1977.

TABLE 2

PHOTOMETRY AND POSITIONS OF OBJECTS IN THE SURVEY FIELDS

Field	No.	Other Names[a]	R.A.	Decl.	*B*	Field	No.	Other Names[a]	R.A.	Decl.	*B*
S6	8	...	0^{h}39^{m}33^s.12	41° 1′17″.1	19.1	S6	4	...	40^s.90	41° 1′28″.6	20.8
S5	12	...	33.12	40 58 29.8	16.9	S6	3	...	40.82	41 1 9.6	21.1
S6	16	...	33.58	41 0 13.7	21.3	S6	2	...	41.07	41 0 47.1	20.1
S6	9	FJ-y	33.63	41 1 11.9	17.7	S5	2	...	42.53	40 58 4.3	20.2
S5	13	...	33.93	40 58 0.8	18.8	S7	3	...	42.58	40 57 22.1	19.5
S6	7	...	34.08	41 2 10.7	18.6	S5	1	...	42.58	40 58 40.0	19.1
S6	15	...	34.44	41 0 25.8	22.2:[b]	S6	1	...	42.84	41 0 43.7	19.4
S5	11	...	34.59	40 59 34.7	21.2:	S7	2	S8-11	42.93	40 56 53.1	17.3
S7	8	B-86	34.64	40 57 35.4	16.0[c]	S7	4	...	42.93	40 57 48.0	20.3
S6	10	...	35.10	41 1 5.6	20.7	S8	15	...	42.14	40 55 42.0	20.6
S6	14	...	35.56	41 0 36.8	18.1	S8	12	...	43.64	40 56 41.5	21.4:
S5	14	...	35.71	40 57 57.4	21.0	S7	1	S8-10	44.48	40 56 48.5	19.7
S6	11	...	35.97	41 0 59.9	20.9:	S8	13	...	45.17	40 56 0.0	21.4
S7	9	...	36.22	40 57 7.2	20.7	S8	9	...	45.68	40 56 36.8	20.8
S7	11	...	36.52	40 56 34.9	16.7	S8	16	...	46.24	40 55 9.3	19.4
S6	12	FJ-x	36.58	41 0 51.8	17.4	S8	8	...	46.24	40 56 57.1	21.7
S5	10	...	36.63	40 59 48.0	19.8	S8	18	...	46.75	40 56 22.6	21.7:
S7	13	...	36.93	40 56 42.9	21.4:	S8	14	B-106	46.85	40 55 51.9	17.2
S6	17	...	37.39	41 0 6.3	21.0	S8	6	...	46.90	40 57 8.0	19.0
S5	15	S7-7	37.41	40 57 53.5	19.6	S8	7	...	46.95	40 56 53.0	20.2
S5	9	...	37.54	40 59 26.7	21.9:	S8	5	FJ-q	47.36	40 57 10.9	16.9
S7	12	...	37.95	40 56 35.4	20.6	S8	4	...	47.61	40 57 1.6	19.6
S6	13	...	37.61	41 0 55.2	20.4	S8	19	...	47.66	40 55 35.2	21.4
S5	8	...	38.66	40 59 34.7	20.1	S8	17	...	47.86	40 55 10.5	19.2
S5	6	...	38.66	40 59 12.8	20.5	S8	3	B-114	50.15	40 56 18.4	18.0
S7	17	...	38.71	40 56 6.7	20.9	S8	2	...	50.56	40 55 24.3	18.4
S7	18	...	39.02	40 55 49.9	18.2	S8	1	...	51.32	40 55 16.8	20.2
S7	6	...	39.07	40 57 24.5	20.9	S9	11	...	55.91	40 56 7.3	20.2
S6	5	...	39.58	41 1 44.8	20.6	S9	13	...	58.74	40 54 37.4	20.4
S5	5	...	39.68	40 58 58.4	20.1	S9	10	...	58.85	40 56 12.5	20.2
S7	10	...	39.83	40 57 59.0	20.0	S9	12	...	58.90	40 54 52.4	20.8
S5	4	FJ-m; FJ-z2	39.88	40 58 29.0	16.2[c]	S9	8	...	59.15	40 55 36.8	17.3
S6	6	...	39.89	41 2 7.9	21.4:	S9	9	B-126	59.61	40 56 16.5	18.0
S5	3	...	39.93	40 58 20.4	20.1	S9	7	...	0^{h}40^m 0.02	40 55 19.5	18.4
S7	15	...	39.98	40 56 19.4	20.6	S9	6	...	1.59	40 55 23.0	20.5
S6	10	...	39.99	41 0 33.4	18.1	S9	5	...	2.30	40 55 15.5	20.3
S5	7	...	30.14	40 59 38.1	19.1	S9	3	...	2.86	40 55 42.6	17.6
S7	5	...	40.39	40 57 15.8	18.9	S9	4	B-128	3.67	40 54 47.2	17.9
S7	14	B-D53	40.44	40 56 16.4	19.4	S9	2	...	4.54	40 55 43.7	19.2
S7	16	...	40.79	40 56 9.0	20.7	S9	1	...	5.56	40 55 35.1	18.9[d]

© American Astronomical Society • Provided by the NASA Astrophysics Data System

1985ApJ...290..140W

TABLE 2—*Continued*

Field	No.	Other Names[a]	R.A.	Decl.	*B*	Field	No.	Other Names[a]	R.A.	Decl.	*B*
S10	9	...	5^{s}99	40°56′ 1.″4	19.3	S4	17	...	20^{s}.75	40°58′24.″3	20.4
S2	12	B-262	6.00	41 3 1.8	18.7	S4	20	...	20.80	40 57 45.2	20.6
S10	7	...	6.04	40 57 10.5	18.4	S4	21	...	20.85	40 57 38.3	22.3:
S10	8	FJ-a	6.65	40 56 6.0	16.6[c]	S4	16	...	20.95	40 58 1.9	19.4
S2	13	FJ-h	6.92	41 1 32.0	16.7[c]	S4	18	...	21.10	40 58 35.8	20.3
S10	6	...	7.36	40 57 7.1	18.6	S3	13	...	21.45	40 59 32.6	17.6
S2	14	...	9.11	41 1 51.5	21.3:						
S2	11	B-136	9.41	41 3 9.1	17.8	S4	15	...	21.71	40 58 21.5	18.0
S10	10	...	9.91	40 55 49.9	20.7	S3	7	...	21.75	41 0 26.7	20.6
S10	5	...	10.31	40 56 41.2	19.5	S4	14	...	22.48	40 58 46.8	17.0
						S4	8	...	22.48	40 56 42.4	20.0
S2	10	B-138	11.35	41 2 9.4	18.0	S1	6	...	22.59	41 3 4.8	17.7
S10	11	...	11.68	40 55 34.9	20.7	S4	9	...	22.73	40 57 19.3	16.6
S10	4	...	11.79	40 56 18.7	18.8	S3	6	...	22.77	41 0 30.2	20.5
S2	9	B-139	12.16	41 1 56.2	18.4	S4	10	...	23.24	40 57 23.9	26.0
S2	8	B-D84	12.21	41 1 46.3	19.5	S1	5	...	23.30	41 2 55.0	20.4
S2	7	...	12.57	41 1 48.7	21.2	S1	1	...	23.70	41 1 52.3	18.7
S10	3	...	12.86	40 56 19.3	19.0						
S2	6	...	13.33	41 1 14.7	18.1	S3	5	M31C-204	23.79	41 0 27.3	16.6
S10	2	...	13.97	40 57 18.6	17.9	S4	11	...	24.10	40 58 10.0	20.4
S2	4	FJ-a	15.06	41 2 22.1	16.7[c]	S4	7	...	24.31	40 56 42.9	19.9
						S4	13	...	24.56	40 58 36.4	20.9
S2	3	...	15.31	41 1 40.0	19.6	S1	3	...	24.72	41 1 20.6	20.6
S2	5	B-143	15.37	41 2 53.1	17.1	S4	12	...	25.07	40 58 30.1	20.5
S10	12	...	15.50	40 57 27.2	20.3	S1	4	...	25.54	41 2 34.9	18.7
S2	2	...	16.54	41 1 19.8	17.2	S1	2	FJ-d; B-152	25.69	41 1 49.9	17.1
S10	1	...	16.87	40 56 20.4	16.2	S4	4	...	26.19	40 57 48.0	20.5
S1	9	S2-1; FJ-b	16.91	41 2 50.1	16.6[c]	S4	3	B-153	26.29	40 58 24.9	17.1
S3	10	...	17.17	41 0 21.5	20.3						
S3	9	...	17.73	41 1 0.1	18.8	S3	3	...	26.33	41 0 31.8	19.0
S1	8	...	18.82	41 1 31.5	19.9	S3	2	...	26.59	41 0 16.4	16.3[c]
S3	8	...	19.16	41 0 55.5	19.7	S3	4	...	26.74	41 0 45.7	20.0
						S4	5	...	26.90	40 56 58.5	21.2:
S1	7	B-148	19.53	41 1 39.6	16.7	S4	6	...	26.90	40 56 55.1	21.2:
S4	22	...	19.58	40 57 29.6	20.2	S3	1	B-154	28.16	40 59 38.3	18.1[d]
S3	11	.	19.87	41 0 10.0	20.5	S4	1	...	28.98	40 57 46.9	16.3[c]
S4	19	...	19.98	40 58 40.4	20.1	S4	2	...	29.14	40 58 41.6	19.6

[a] Other names: B = Battistini *et al.* 1980. FJ = Ford and Jacoby 1978. M316 = Sargent *et al.* 1977.
[b] A colon indicates that image is too faint.
[c] Image is saturated.
[d] Image near edge of field.

The dust features in Figure 3*b* show very clearly the striking feature pointed out by Johnson and Hanna (1972): the dust lanes extend to within seconds of arc of the nucleus. Our computer-enhanced frame reproduces most of the features seen in Johnson and Hanna's photographically enhanced Figure 1. Our data are somewhat deeper than Johnson and Hanna's and show features even closer to the nucleus than their photo. We will return to a detailed study of the dust and a comparison with the work of Hodge (1980) and Gallagher and Hunter (1981) in a future paper.

This smoothing and subtraction was done for all three central fields in all filters. The resulting E and W fields are shown in Figures 4*a* and 4*b*. The standard 2CAP simulated aperture photometry routine was then used to produce photometry using a 2.″5 aperture and 5″–9″ sky annulus. The results were found to be quite reproducible and consistent from one exposure to another. Table 3 is a summary of this photometry for the 49 detectable images in the central fields (limiting magnitude ~21). The numbers assigned to the stellar images refer to the finding charts in Figure 5. The statistical uncertainty in most of these magnitudes is in the range 0.01–0.07 mag, depending on image brightness. However, because of poorly determined transformation equations, systematic effects produced by the processing of the central frames, and the rather severe spatial undersampling problem (because of exceptionally good seeing, image size was often $\lesssim 2$ pixels, and with roughly 10% dead space between pixels in one direction, the centering of the image with respect to the detector grid led to variations in the signal of close to 0.1 mag), the error in the stated magnitudes is probably closer to ± 0.2. An additional source of error in the final sample of object magnitudes arises from the difference in the aperture sizes used in the central and survey fields. Because of the finite size of the image of a typical globular cluster, there may be up to 0.15 mag (for the case of a compact cluster with core radius close to 1″) systematic difference between the magnitudes of the central and survey fields. After our reduction of data was completed, we received a preprint from Buonanno *et al.* (1982) which lists magnitudes for M31 globular clusters in the Bologna survey (Battistini *et al.* 1980). The overlap of our Table 3 with their sample is six objects. In all but one of these objects our *B* magnitudes agree with theirs to less than 0.1 mag, which is within our errors.

A few images have particular problems in photometry and are so noted in the tables. There are three principal sources of possible major photometric errors. The brightest images saturate the videocamera and have bad values for intensity in their

© American Astronomical Society • Provided by the NASA Astrophysics Data System

1985ApJ...290..140W

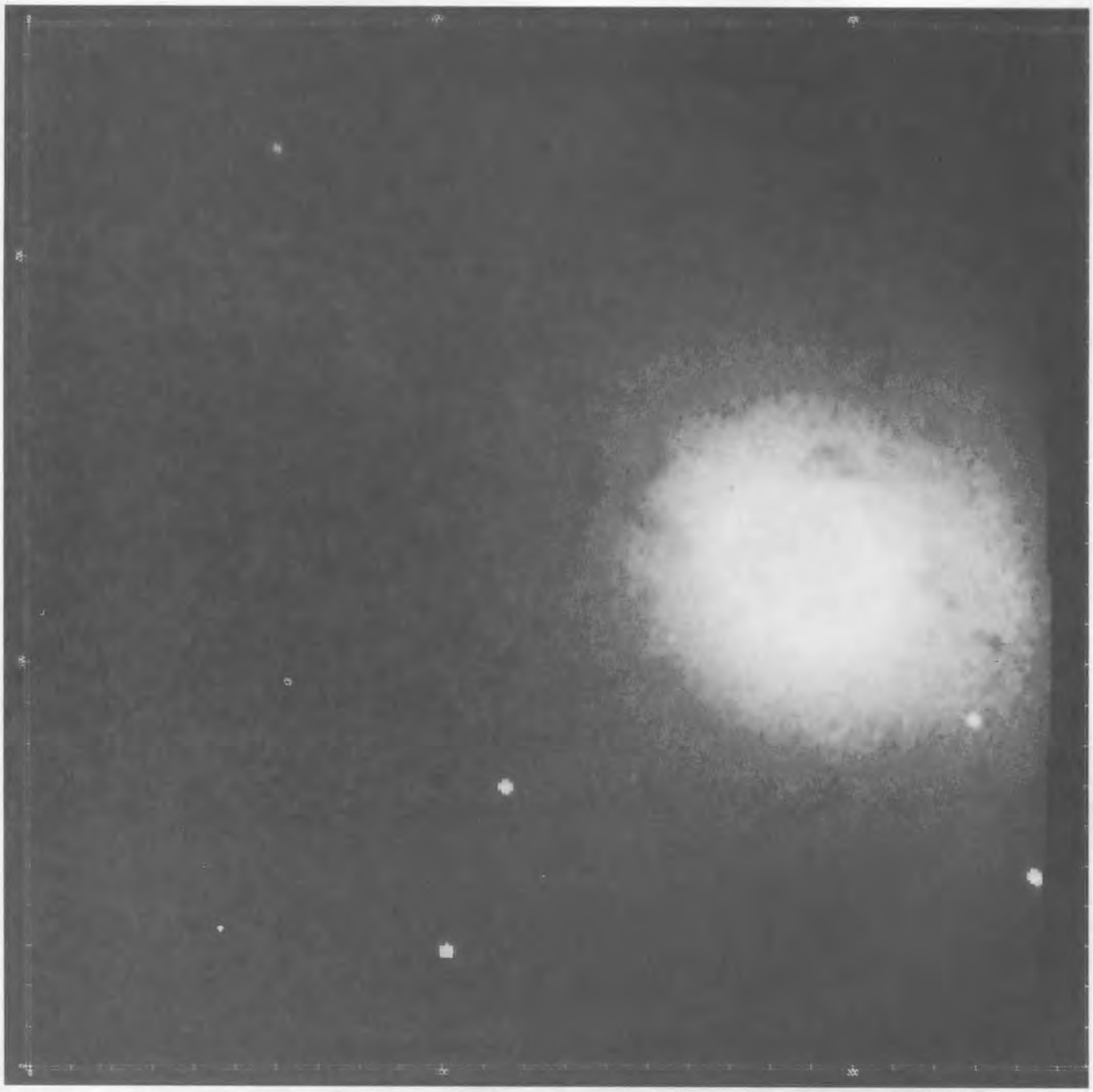


FIG. 3a.—The central frame (C) before subtraction of the bulge light. This picture is comparable to the best published photographs of the bulge region of M31.

© American Astronomical Society • Provided by the NASA Astrophysics Data System

1985ApJ...290..140W

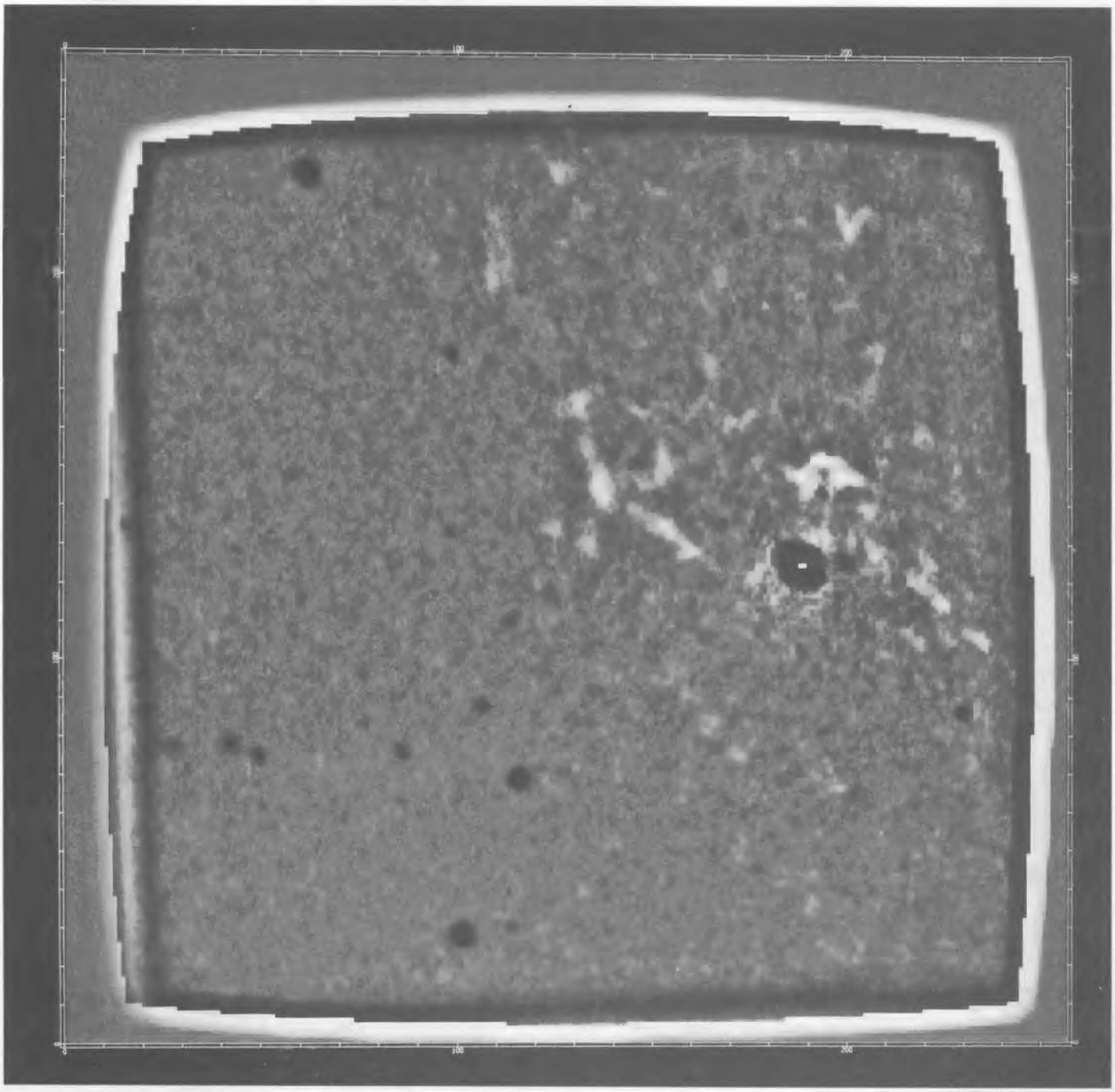


FIG. 3*b*.—The same frame after removal of the bulge. Note the many stellar images and the detailed dust distribution. Compare with the photographic technique of Johnson and Hanna (1972).

© American Astronomical Society • Provided by the NASA Astrophysics Data System

1985ApJ...290..140W

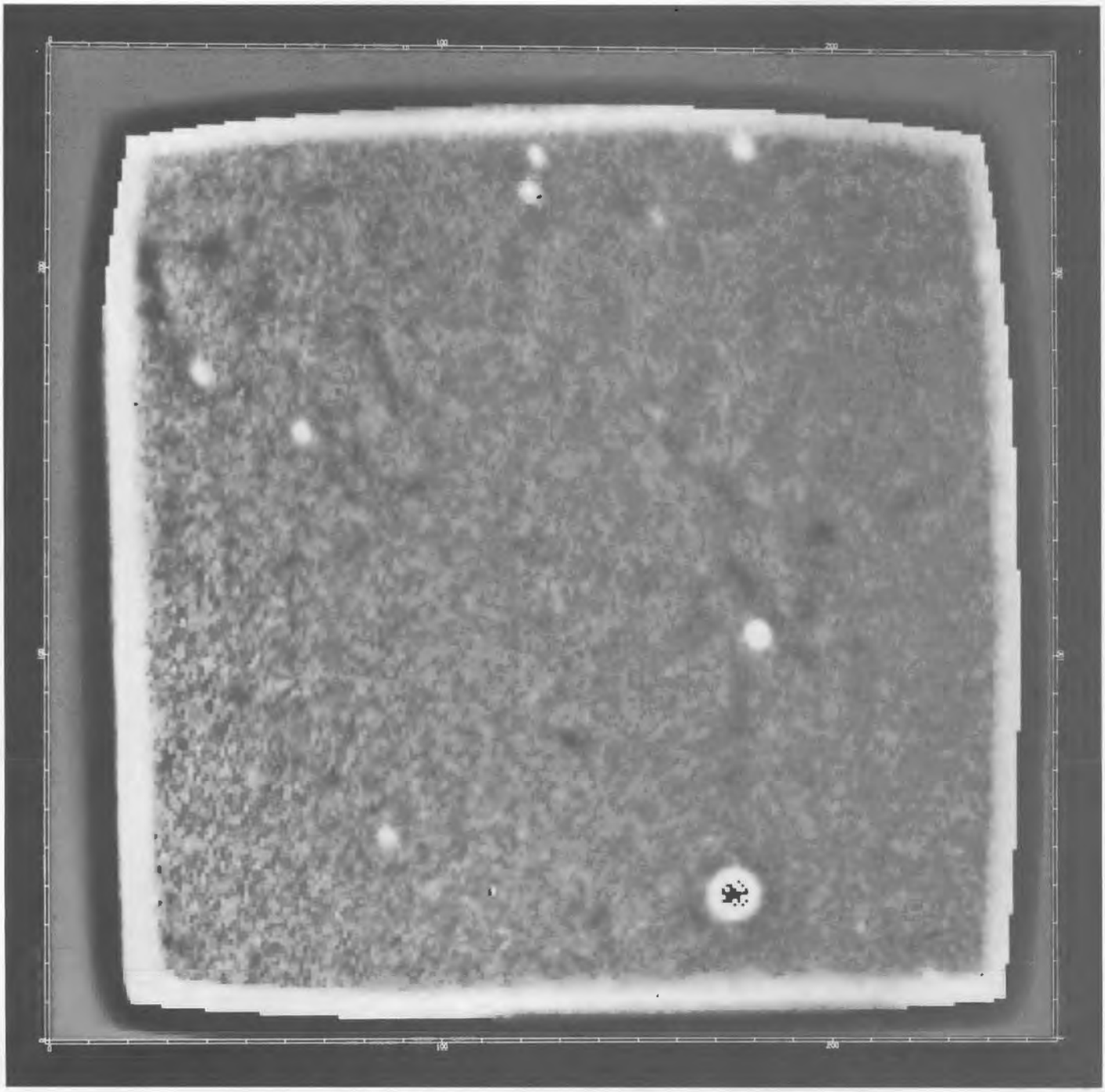


FIG. 4*a*.—Frame W with the bulge removed

© American Astronomical Society • Provided by the NASA Astrophysics Data System

1985ApJ...290..140W

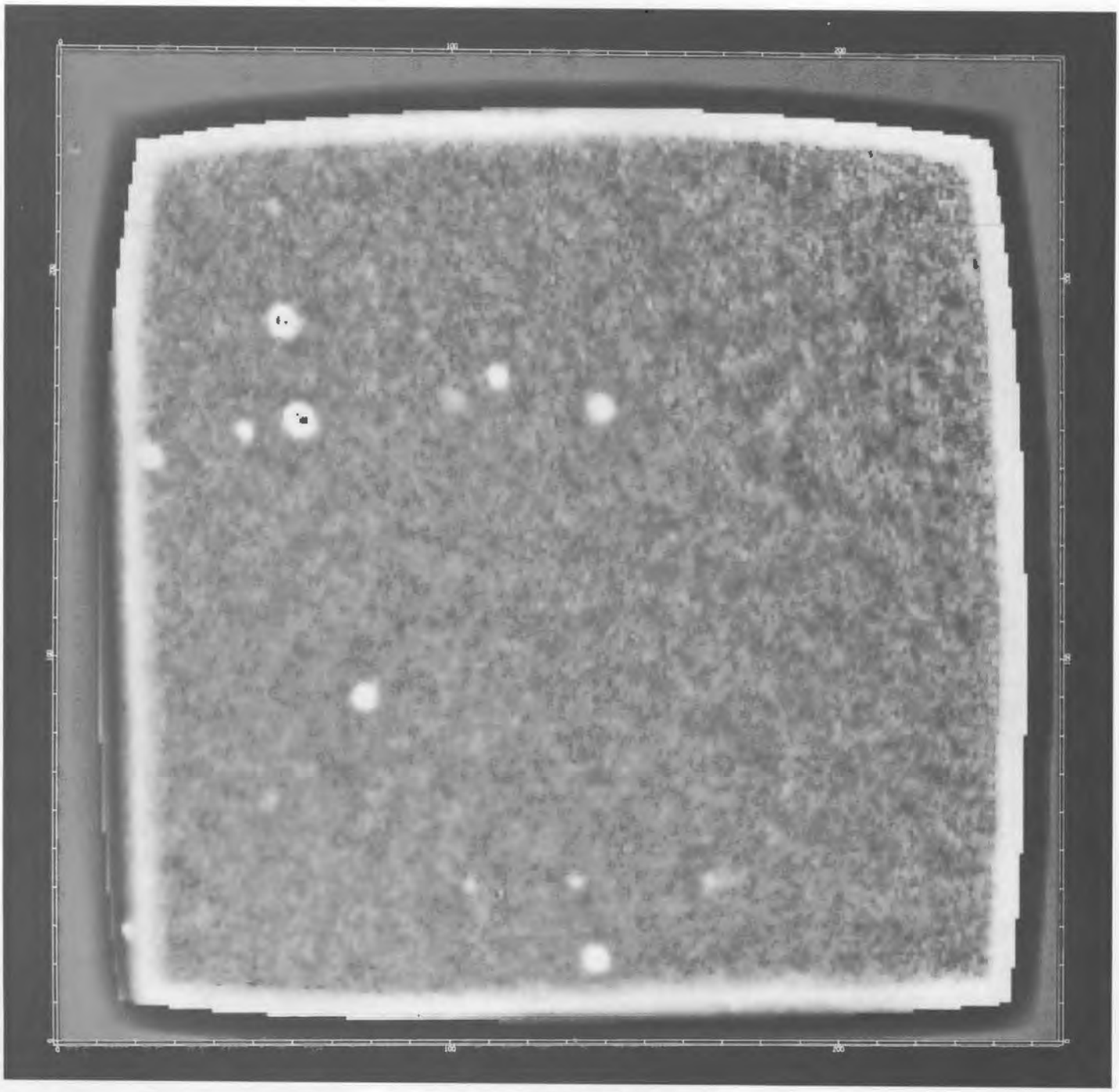


FIG. 4*b*.—From frame E with the bulge removed

© American Astronomical Society • Provided by the NASA Astrophysics Data System

1985ApJ...290..140W

TABLE 3

PHOTOMETRY AND POSITIONS OF OBJECTS IN THE THREE CENTRAL FIELDS

FIELD	No.	OTHER NAMES[a]	1950 COORDINATES R.A.	Decl.	B	B−I
W	1	FJ-l	$0^h39^m48^s.9$	41° 0′ 3″	16.7	1.6
W	2	B-112	49.1	41 1 16	17.7[b]	2.7
W	3	FJ-k	49.2	40 59 24	~>15.0[c]	[d]
W	4	...	50.3	41 1 5	19.7	2.3
W	5	B-261	51.9	41 1 14	18.8[b]	1.6
W	6	B-119	52.0	41 1 9	18.5	2.3
W	7	...	53.7	40 59 33	18.6	1.6
W	8	...	54.9	41 0 33	18.3	2.3
W	9	...	55.4	40 59 41	<20.0[e]	[d]
W	10	...	56.0	41 0 57	18.5	1.0
C	1	LF-d	58.0	40 59 21	17.7	0.6
C	2	...	59.5	40 59 44	~18.0?	[d]
C	3	...	59.8	40 59 55	...	[d]
C	4	nucleus	0^h40^m 0.0	40 59 43	[c]	[d]
C	5	...	0.9	41 00 34	<19.0	[d]
C	6	...	2.0	40 59 23	<19.0	[d]
C	7	...	3.3	40 59 39	<19.0	[d]
C	8	FJ-e, LF-a	3.7	40 59 12	15.8	1.0
C	9	...	3.9	40 59 35	<19.0	[d]
C	10	...	3.9	40 58 49	<19.0	[d]
C	11	...	4.2	40 59 23	18.7	1.2
C	12	...	4.5	41 00 03	<19.0	[d]
C	13	B-D75, A-B1, LF-c	4.5	40 58 48	15.3	1.7
C	14	...	4.6	41 00 15	18.8	1.0
C	15	...	4.6	40 59 49	...	[d]
C	16	...	5.2	40 59 16	18.4	1.3
C	17	B-131, FJ-f, A-C1	6.5	41 00 42	16.3[b]	2.1
C	18	...	6.6	40 59 56	<19.0	[d]
C	19	B-132	7.1	40 59 15	18.7	1.5
C	20	...	7.4	40 59 18	18.6	2.8
E	1	...	9.8	40 58 55	19.4	1.3
E	2	B-D80	10.1	40 59 47	18.8	0.1
E	3	...	11.4	40 58 8	20.5	2.2
E	4	...	13.4	40 59 38	20.2	1.3
E	5	...	14.2	40 58 29	19.8	1.6
E	6	B-144	15.6	40 59 39	18.1	1.5
E	7	...	15.7	40 58 18	17.5	1.1
E	8	...	15.9	40 58 30	21.2	2.4
E	9	B-D90, S3-17	17.0	40 59 44	18.7	1.6
E	10	...	17.2	40 58 50	<20.0	[d]
E	11	...	17.3	40 58 29	20.1	1.5
E	12	...	17.3	40 58 40	<20.0	[d]
E	13	S3-16	17.5	40 59 40	20.0	1.6
E	14	...	18.2	40 58 46	<20.0	[d]
E	15	...	18.6	40 58 38	<20.0	[d]
E	16	B-146, S3-18	18.7	40 58 57	18.3	1.6
E	17	FJ-xx, S3-15	19.5	40 59 38	16.7	[d]
E	18	S3-12	19.7	40 59 53	16.7	[d]
E	19	S3-14	20.3	40 59 35	19.1	[d]

[a] Other names: B = Battistini *et al.* 1980. JF = Ford and Jacoby 1978. A = Alloin, Pelut, and Bijaoui 1976. LF = Lawrie and Ford 1982. S3 = Image also in survey field 3 (see Table 3). M31C = Sargent *et al.* 1977.

[b] Image near edge of field.

[c] Image is saturated.

[d] Image too near nucleus.

[e] < = image too faint.

© American Astronomical Society • Provided by the NASA Astrophysics Data System

1985ApJ...290..140W

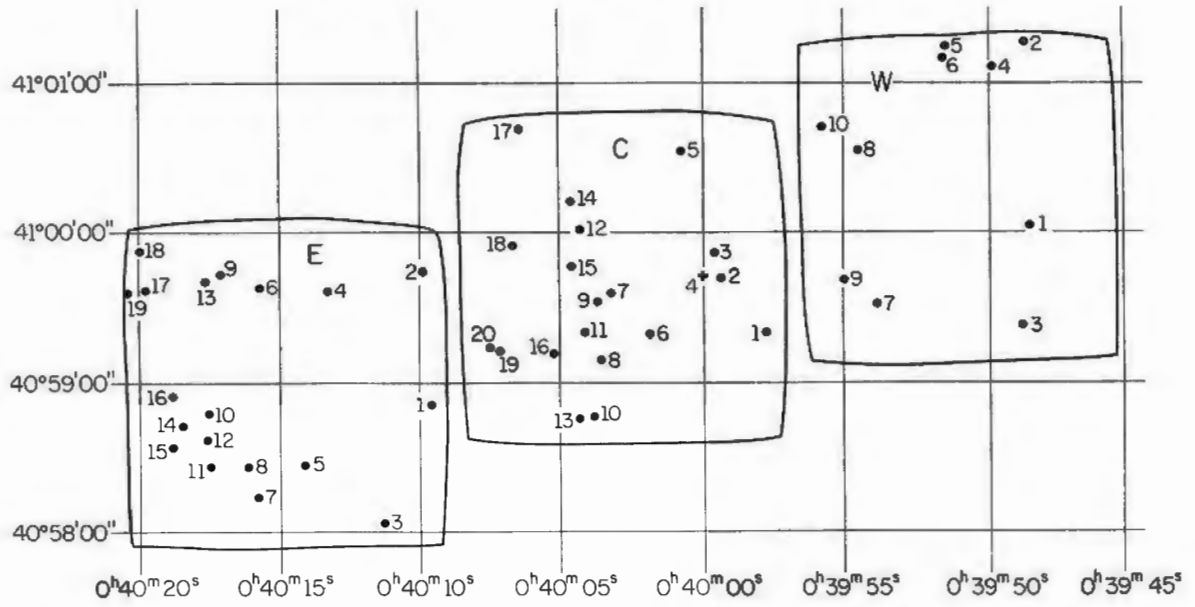


FIG. 5.—An accurate finding chart for stellar images on frames W, C, E. The numbers refer to the entries of Table 3.

central pixels. The software does not take this into account when integrating the image. Some images were very near the ends of the videocamera frames. It is likely that the magnitudes given are in error because of faulty background subtraction. Finally, the very faintest images are difficult for the software to sort out from the sky. Their photometric values are quite suspect and are often given as upper limits in Table 3.

c) Positions

The R.A. and decl. of all optical fields were fitted by computer at the Harvard-Smithsonian Center for Astrophysics by Leon Van Speybroeck. In each field, the R.A. and decl. for known Bologna globular clusters (Battistini *et al.* 1980) and astrometric reference stars (Ford-Jacoby 1978; Lawrie and Ford 1982) were used as input positions. A fit was made using the known scale of 0.″57 per pixel to convert (x, y) pixel number to (R.A., decl.) coordinates. The residuals in most cases were 1″ or less. The positions in survey fields 4 and 10 were determined with only one input each, and those of survey fields 7 and 9 had only two inputs, so one should be careful in using those coordinates. The resulting positions in Tables 2 and 3 provide a reference grid for future work on M31's bulge, such as performing coincidence searches with X-ray sources (Paper II).

IV. THE "MISSING" BULGE GLOBULAR CLUSTERS

There has been a long effort to detect the globular clusters in M31. The two most extensive recent surveys were those of the "M31 consortium" (Sargent *et al.* 1977) and the Bologna group (Battistini *et al.* 1980; Buonanno *et al.* 1982). Since the latter is more recent, we will make most of our comparisons with them. The situation is extensively reviewed by Harris and Racine (1979). There are two major results of interest to us: the radial distribution of globular clusters and their luminosity distribution.

The radial projected density of globular clusters increases toward the center as a $R^{1/4}$ de Vaucouleurs law (de Vaucouleurs and Buta 1978; Harris and Racine 1979). However, as shown by the points in our Figure 9 (taken from Harris and Racine 1979), is a flattening of the density profile inside 4 kpc (20′). This does not happen in our Galaxy (compare Figs. 1 and 6 of de Vaucouleurs and Buta 1978 and Fig. 8 in Harris and Racine 1979). Harris and Racine conclude that part of this flattening is real. This led to the question of whether these central globular clusters are "missing." Some theoretical models (Tremaine, Ostriker, and Spitzer 1975; Tremaine and Ostriker 1982) envision the nucleus of M31 (Light, Danielson, and Schwarzschild 1974) as being composed of stars from disrupted bulge globular clusters which spiraled by dynamical friction, thus depleting the numbers of globular clusters in the inner bulge.

The luminosity distribution of globular clusters in M31 is still uncertain because of incompleteness. However, there is general agreement that it is similar to the Galaxy's, with a peak at $M_v \sim -7.3$ with a standard deviation of ~ 1.2 (Racine and Shara 1979; Harris and Racine 1979; Battistini *et al.* 1980). Using the average $B-V \approx 0.8$ for M31 globular clusters (Harris and Racine 1979, their Fig. 3), a distance modulus of 24.4 (de Vaucouleurs and Buta 1978), and a reddening $A_B \approx 0.4$, this implies we should detect globular clusters in our blue survey in the range $15.7 < B < 20.9$. Since our limiting magnitude is $M_B \approx 21$, we should be able to detect most of the M31 bulge globular clusters in our fields.

The question is then, how do we tell if our optical images are globular clusters? Previous surveys relied on image morphology. For instance, the M31 consortium (Sargent *et al.* 1977) selected by eye those "compact, almost stellar images, with a definite diffuse border" as their globular cluster candidates. The Bologna group differentiated their candidates from stars by the greater image spread found in globular clusters. Both of these methods agree that there is a deficiency of globular clusters in the general bulge region. These techniques are very reasonable approaches to the problem of searching for globular clusters. For typical galactic globular clusters at the distance of M31, we would expect a range in image size (FWHM of about 2 core radii, Peterson and King 1975) of 0.″4–1.″2. Thus, in good seeing conditions, the larger clusters will be clearly resolved. However, some fraction of the clusters will appear stellar even in moments of exceptional seeing.

© American Astronomical Society • Provided by the NASA Astrophysics Data System

1985ApJ...290..140W

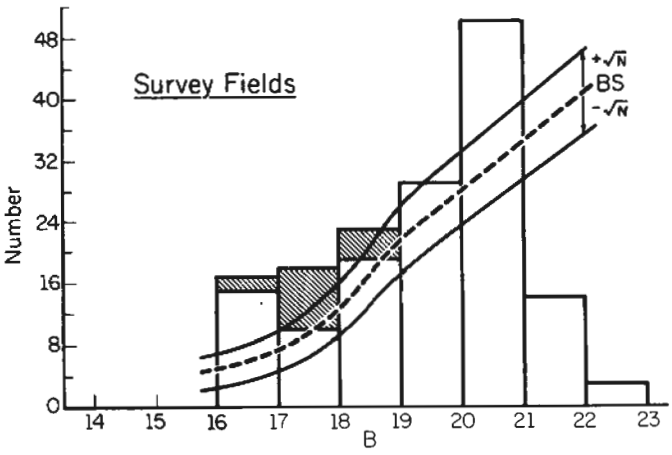


FIG. 6a

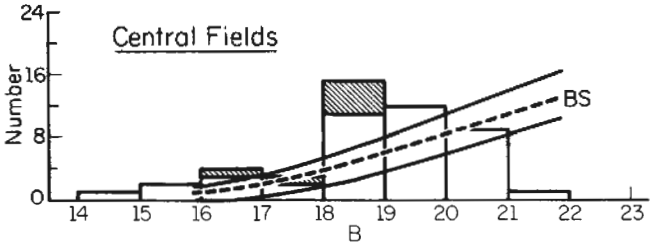


FIG. 6b

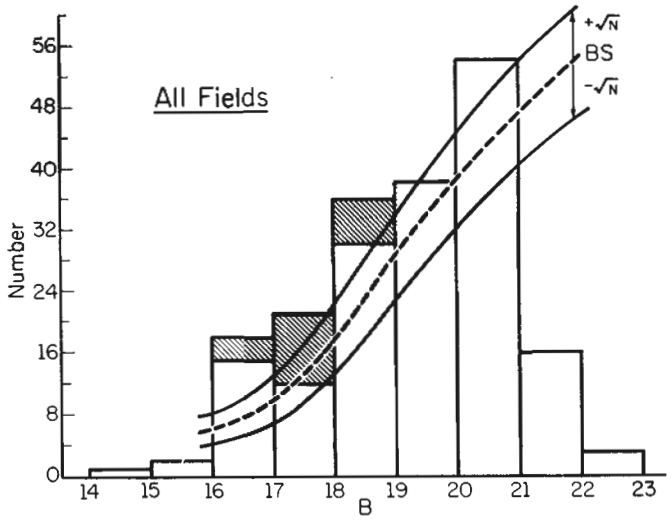


FIG. 6c

FIG. 6.—(*a*) The 154 stellar images in the 10 survey fields binned by apparent blue magnitude. Also shown is the BS model of foreground galactic stars. Lines indicating the statistical uncertainty of the BS model are included (see text). (*b*) The same as Fig. 6*a* for the central fields. (*c*) The same as Fig. 6*a* for the combined 195 images in all 13 fields.

Our method does not utilize image morphology. We rely on M31's globular clusters to produce an excess of bright images in the bulge region over the normal galactic foreground star counts. Fortunately, there now exists a theoretical model of the density of stellar images in a given magnitude range expected at a given galactic latitude and longitude (Bahcall and Soneira 1980, hereafter the BS model). We use their numbers appropriate for M31 ($b = 21.^{\circ}7, l = 121^{\circ}$). The accuracy of their model is quoted as 15% when compared with observations.

In Figure 6*a* we give a histogram of the 154 B magnitudes from the 10 survey fields. The bins are 1 mag wide. The 14 known (Battistini *et al.* 1980) globular clusters in our 10 fields are shown by shading. The BS model for galactic foreground stars is plotted after adjusting to the $10 \times (140'')^2 \approx 0.015$ deg^2 in our survey fields. Above and below the BS model line are lines indicating BS + $N^{1/2}$ and BS − $N^{1/2}$. A similar histogram for the three central fields is shown in Figure 6*b* and for the combined 13 fields in Figure 6*c*. All stars that overlapped between the fields have been removed in the combination.

It is clear that there are excess stellar images over the predicted foreground star counts. Further, these excesses are significant at the 1–3 sigma level *per bin*. Over the range from $B = 16.0$ to $B = 20.9$, the BS model predicts 121 stars, with dispersion of 11, while we observe 182 images, an excess of 61 objects. This is clearly a significant excess of images. The excess counts are binned in Figure 7. The histogram peaks at the appropriate value, with the appropriate width for M31 globular clusters. The 19 known globular clusters are all contained in our excess image bins. We therefore tentatively conclude that our optical images contain ~20 new candidates for the "missing" globular clusters down to a blue magnitude limit of 20.

Several features of our results should be noted. First, in the survey fields (Fig. 6*a*), it is the *brighter* magnitudes at which most of our new candidates are found. Also, we are far enough away from the nucleus that the bulge light is not a major problem. We can only conclude that our candidates are quite compact globular clusters which are intrinsically bright ($M_B \approx -8.5$). An example of such a cluster in our Galaxy is M15. Second, the globular clusters in the central bulge fields are systematically less luminous than in the survey fields. This may be caused by the anticipated tidal stripping of globular clusters near the nucleus of M31 or by systematic errors in our photometry. Finally, the peak of excess optical images in the survey fields at $20 < B < 21$ probably is partially caused by luminous ($M_v \sim -5$) B stars in the inner disk of M31. Spectra of these candidates to sort out the luminous stars would complement Humphreys's studies of luminous stars in the Local Group (e.g., Humphreys 1979). Note that this peak is not seen in the three central fields; this is expected, since these fields do not intersect the wide ring of young population objects in M31's disk.

There is further evidence that this excess of bright images is real, and that the BS model correctly predicts the density of foreground stars. This support comes from the star counts presented in Figure 1. Since the limiting magnitude of these counts is ~18, the brighter peak of excess images shown in Figure 6*c* should be included. Counts of stellar images were done over the whole 55′ field of the telescope. Outside the central $r \sim 10'$ region, the density of images was quite uniform. Subtraction of this background level revealed an excess of ~30 images within a central region of ~150 arcmin^2 of M31, in fair agreement with the excess number above $B \sim 18.0$ calculated from the videocamera data using the BS model.

© American Astronomical Society • Provided by the NASA Astrophysics Data System

1985ApJ...290..140W

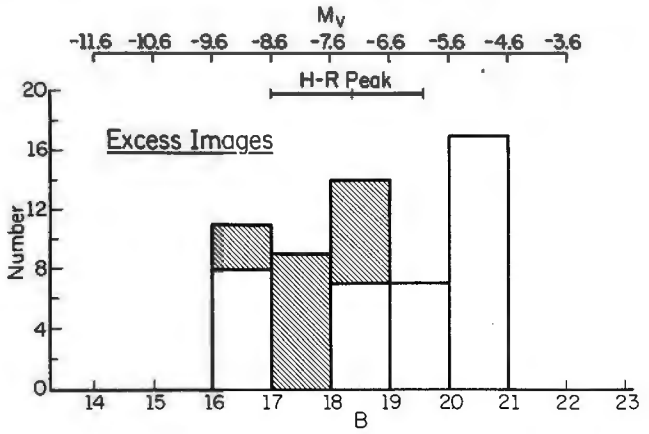


FIG. 7.—Histogram of optical images minus the BS model. This gives the excess images which should be intrinsic to M31. The peak ±1 standard deviation of the Harris-Racine (1979) luminosity distribution for M31 globular clusters is shown. The scale at the top is the estimated V absolute magnitude of these excess images.

This broad statistical argument can be further checked in the central fields, because there we have two-color photometry. This allows us to construct the color-magnitude diagram for the objects in the central fields (Fig. 8). The majority of objects lie in the color range typical of galactic globular clusters ($1.2 < B-I < 2.5$; Kron and Mayall 1958). However, since we would expect foreground K stars to inhabit the same region of the diagram, color alone is not a sure discriminator of globular clusters. Nonetheless, the color-magnitude diagram indicates that it is plausible that our excess images are globular clusters. There exist at least two ways to determine the true nature of the excess images. One is to obtain radial velocities. A program to do just that has been initiated at Whipple Observatory. The other is to examine the small-scale structure and the images. Data obtained with ~0.″5 seeing with a linear detector should allow the detection of most globular clusters.

Finally, if the projected surface density of these suspected globular clusters is compared with the inward extrapolation of the $R^{1/4}$ law observed for the surface density of globular clusters in the outer parts of M31 (Harris and Racine 1979), excellent agreement is seen. This is shown in Figure 9. The previously known data are reproduced from Harris and Racine (their Fig. 8) and represent their reanalysis of the counts of Sargent *et al.* (compare de Vaucouleurs and Buta 1978). The de Vaucouleurs law fit is the one given for M31 by Harris and Racine (1979). The flattening of the density profile is clearly seen. Again, Harris and Racine (1979) conclude that although part of this effect is caused by the inability to see globular clusters against the rising bulge light, part of it must be real. They state that "the central regions would have *many easily detectable bright clusters* if the incompleteness fraction were as high" as their curve indicates (emphasis added).

In Figure 9 we plot two points derived from our survey fields and central fields. The inner point represents the density of known globular clusters plus our excess images in the three central fields. These images are all within 4′, or 800 pc, of the nucleus. This disk has an area of 2 kpc^2, of which one-third is covered by our fields W, C, and E. In these fields (from Fig. 6*b*) are six known globular clusters and ~12 candidates, for a density of ~27 objects per kpc^2. We plot this density at a radius whose enclosed area is one-half that of the 4′ circle. Likewise, all 13 fields are within a 6.′5, or 1.3 kpc, radius circle, of which one-half is covered by our fields. There are (from Fig. 6*c*) 19 known clusters and ~20 candidates in our fields, for a density of 14 objects per kpc^2. Again, this value is plotted at the half-area radius. In particular, our counts indicate that there may be ~40 bright objects in the central 6.′5 radius.

We may then ask why all previous surveys (cf. Battistini *et al.* and references therein) for globular clusters in M31 agree that there is a deficiency in the central regions. We suggest that this

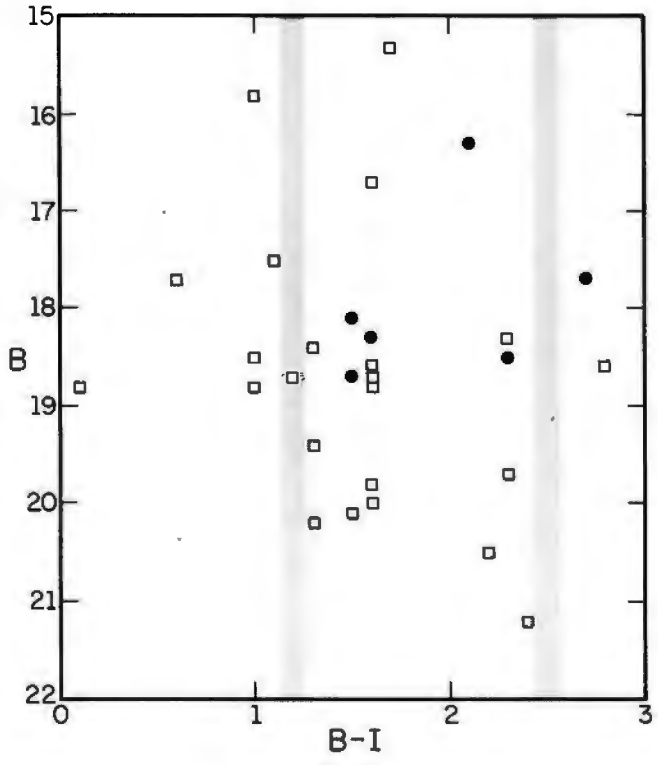


FIG 8

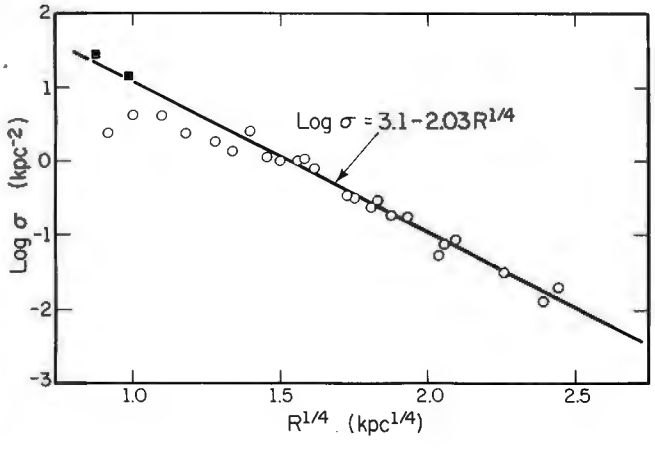


FIG 9

FIG. 8.—A color-magnitude plot (B vs. $B-I$) of the stellar images in the three central fields. The known globular clusters are shown as filled circles.

FIG. 9.—The logarithm of the surface density of globular clusters in M31 as determined by Harris and Racine (*circles*) fitted to a de Vaucouleurs $R^{1/4}$ law. Our data are represented by the squares, indicating that we have found the missing globular clusters in M31.

© American Astronomical Society • Provided by the NASA Astrophysics Data System

1985ApJ...290..140W

deficiency may be due to a selection effect. In these previous surveys, image morphology was the primary criterion used to separate globular and nonglobular images. In the region of interest, the background visual survey brightness ranges from ~ 20 mag arcsec^{-2} to 15 mag arcsec^{-2} (Burgess 1976). It seems unlikely that extension of images on photographic plates can be detected at levels below $\sim 5\%$ of the background (Latham 1974), i.e., below 23 to 20 mag arcsec^{-2} for the range of bulge surface brightness encountered. If a globular cluster such as NGC 6541 is placed on this background, its apparent radius to 5% of background ranges from 0".8 to 3".0 (depending upon its distance from the nucleus), based on the data of Williams and Bahcall (1979). Clearly, plates taken under typical seeing conditions ($\sim 2''$) will not allow detection of some fraction of the clusters near the center of M31 by means of image morphology. An additional effect that may be important is the tidal truncation of globular clusters near the center of M31, reducing their apparent diameters even further.

V. STELLAR POPULATIONS

It has been suggested recently that some spheroidal stellar systems have experienced star formation in the recent past ($< 5 \times 10^9$ yr) (O'Connell 1980; Gallagher and Mould 1981; Mould and Aaronson 1980). The raw materials for star formation are certainly present. The mass return rate from the old stellar population of the bulge can be estimated to be $\sim 5 \times 10^7\ M_\odot\ \mathrm{Gyr}^{-1}$ (Gallagher and Hunter 1981). There are several star formation models which could produce stars luminous enough to be detected in our survey.

If star formation with a *normal* initial mass function (IMF) is going on continuously at a sufficiently high rate, there will be numerous massive ($M \gtrsim 5\ M_\odot$) blue and red stars luminous enough to be detectable (Humphreys 1979; Becker and Iben 1979). Examination of the color-magnitude diagram for our three central fields, however, reveals that there are no stars bluer than $B-I = 0$ or redder than $B-I = 3$, in agreement with van den Bergh (1981). This would indicate that no stars more massive than $5\ M_\odot$ have formed in the inner bulge in the last few $\times 10^8$ yr.

If intermediate-mass stars ($M \approx 3\ M_\odot$) have been formed in the last $\sim 2.5 \times 10^8$ yr, they may reach sufficient luminosities on the asymptotic giant branch (AGB) to be observable (Iben 1977; Renzini and Voli 1980). It should be noted that the existence of such a luminous AGB phase depends upon metallicity (Becker 1979). There are no stars in our color-magnitude diagram which would be representative of this luminous AGB ($B-I \sim 3$–3.5, $B > 20.5$). We feel that this argument is not as strong as for the massive stars, because this region is close to the limiting I magnitude of the survey, and we might not be detecting the hypothesized AGB stars.

In conclusion, we find no strong evidence for star formation in the central kpc of M31 in the range $1.5\ M_\odot < M < 5\ M_\odot$ during the last 2.5×10^8 yr. This lack of recent formation of stars with $M > 1.5\ M_\odot$ is quite different from the situation observed in NGC 205 (Gallagher and Mould 1981). The existence of many planetary nebulae in the bulge of M31 (Ford and Jacoby 1979; Lawrie and Ford 1982) indicates that evolved stars do exist in this region. Either the planetary nebula ejections are occurring on the red giant branch, or the AGB stars are below our detection limit. As pointed out by Gallagher and Hunter (1981), there exists a problem in disposing, via the process of star formation, of the gas lost by evolved stars in the bulge of M31. Either the IMF of the newly formed stars is quite unusual (fewer massive stars), or the gas does not cool and collapse into stars at all.

VI. CONCLUDING REMARKS

We have presented here, for the first time, accurate photometry for stellar images near the nucleus of M31. This has been made possible by taking advantage of the large dynamic range and linearity of modern, two-dimensional detectors in our data reduction methods. This photometry has led to two interesting results. First, on the basis of a statistical argument, we have identified a number of objects which are, possibly, the "missing" globular clusters the central bulge region of M31. We argue that previous surveys for globular clusters in this region have missed these objects because of the difficulty in detecting the nonstellar nature of an image against the bright background of the bulge of M31. Second, we find no evidence for recent formation of stars with masses greater than $\sim 1.5\ M_\odot$ in the bulge. The evidence against the presence of massive stars ($M > 5\ M_\odot$) is very strong, while the observed absence of luminous AGB stars does not preclude the presence of intermediate-mass stars. This lack of recent star formation may support the idea that the gas lost by evolving stars in spheroidal stellar systems is driven out of those systems by a galactic wind.

We would like to thank the staff at Kitt Peak National Observatory and, in particular, Harvey Butcher, Suzanne Hammond, Doug Tody, and Daryl Wilmarth. Karen Strom provided valuable assistance with data processing on the IPPS. We have also benefited greatly from discussions with and the use of unpublished data from Jay Gallagher, John Hackwell, Diedre Hunter, Leon Van Speybroeck, Steve Strom, S. van den Bergh, G. de Vaucouleurs, and Ron Webbink. We especially thank Leon Van Speybroeck for determining the accurate R.A. and decl. of the stellar objects in Tables 2 and 3. The comments of an anonymous referee have aided us in improving this paper. Finally, we would like to thank S. Strom for exercising his editorial wisdom.

REFERENCES

Alloin, D., Pelut, D., and Bijaoui, A. 1976, *Astr. Ap.*, **50**, 127.
Bahcall, J. N., and Soneira, R. M. 1980, *Ap. J. Suppl.*, **44**, 73.
Battistini, P., Bonoli, F., Braccesi, A., Fusi Pecci, F., Malagnini, M. L., and Marano, B. 1980, *Astr. Ap. Suppl.*, **42**, 357.
Becker, S. 1979, Ph.D. thesis, University of Illinois.
Becker, S., and Iben, I., Jr. 1979, *Ap. J.*, **232**, 831.
Buonanno, R., Corsi, C. E., Battistini, P., Bonoli, F., and Fusi Pecci, F. 1982, *Astr. Ap. Suppl.*, **47**, 451.
Burgess, R. D. 1976, Ph.D. thesis, University of Indiana.
de Vaucouleurs, G., and Buta, R. 1978, *A.J.*, **83**, 1383.
Ford, H., and Jacoby, G. 1979, *A.J.*, **219**, 437.
Gallagher, J. S., and Hunter, D. A. 1981, *A.J.*, **86**, 1312.
Gallagher, J. S., and Mould, J. 1981, *Ap. J. (Letters)*, **244**, L3.
Harris, W. E., and Racine, R. 1979, *Ann. Rev. Astr. Ap.*, **17**, 241.
Hodge, P. W. 1980, *A.J.*, **85**, 376.
Humphreys, R. M. 1979, *Ap. J.*, **234**, 854.
Iben, I., Jr. 1977, in *Advanced Stages in Stellar Evolution*, ed. P. Bovier and A. Maeder (Sauverny: Geneva Observatory), p. 1.
Johnson, H. M., and Hanna, M. M. 1972, *Ap. J. (Letters)*, **174**, L71.
Kitt Peak National Observatory. 1980, *Video Camera/CCD Standard Fields* (Tucson: Kitt Peak National Observatory).
Kron, G., and Mayall, N. U. 1958, *A.J.*, **65**, 581.
Latham, D. W. 1974, in *Methods of Experimental Physics*, Vol. **12A**, ed. N. Carleton (New York: Academic Press), p. 221.
Lawrie, D. G., and Ford, H. C. 1982, *Ap. J.*, **256**, 112.
Light, E. S., Danielson, R. E., and Schwarzschild, M. 1974, *Ap. J.*, **194**, 257.
Mould, J., and Aaronson, M. 1980, *Ap. J.*, **240**, 464.
O'Connell, R. W. 1980, *Ap. J.*, **236**, 430.

© American Astronomical Society • Provided by the NASA Astrophysics Data System

1985ApJ...290..140W

Peterson, C. J., and King, I. R. 1975, *A.J.*, **80**, 427.
Racine, R., and Shara, M. 1979, *A.J.*, **84**, 1694.
Renzini, A., and Voli, M. 1980, preprint.
Sargent, W. L. W., Kowal, C. T., Hartwick, F. D. A., and van den Bergh, S. 1977, *A.J.*, **82**, 947.
Strom, S. E., Forte, J. C., Harris, W. E., Strom, K. M., Wells, D. C., and Smith, M. G. 1981, *Ap. J.*, **245**, 416.
Tremaine, S., and Ostriker, J. P. 1982, *Ap. J.*, **156**, 435.
Tremaine, S., Ostriker, J. P., and Spitzer, L. 1975, *Ap. J.*, **196**, 407.
van den Bergh, S., 1981, private communication.
Van Speybroeck, L., Epstein, A., Forman, W., Giacconi, R., Jones, C., Liller, W., and Smarr, L. 1979, *Ap. J. (Letters)*, **234**, L45.
Williams, T. B., and Bahcall, N. A. 1979, *Ap. J.*, **232**, 754.

T. L. BRUNO: Optron Systems, 118 Clark St., Newton Centre, MA 02159

L. L. SMARR: Department of Astronomy, University of Illinois, Urbana, IL 61801

ALLAN WIRTH: Adaptive Optics Associates, 2336 Massachusetts Ave., Cambridge, MA 02140

© American Astronomical Society • Provided by the NASA Astrophysics Data System